NJC

PAPER

View Article Online
View Journal | View Issue

Cite this: *New J. Chem.*, 2014, **38**, 1062

Phosphine derivatives of ciprofloxacin and norfloxacin, a new class of potential therapeutic agents†

Aleksandra Bykowska,[a] Radosław Starosta,*[a] Urszula K. Komarnicka,[a] Zbigniew Ciunik,[a] Agnieszka Kyzioł,[b] Katarzyna Guz-Regner,[c] Gabriela Bugla-Płoskońska[c] and Małgorzata Jeżowska-Bojczuk*[a]

Received (in Montpellier, France) 9th October 2013,
Accepted 22nd November 2013

DOI: 10.1039/c3nj01243c

www.rsc.org/njc

In this paper a new series of chalcogenides of diphenylmethylaminophosphine derived from ciprofloxacin (PPh_2CH_2Cp) and a new phosphine derived from norfloxacin (PPh_2CH_2Nr) are presented. The synthesized compounds were characterized by NMR, MS and X-ray techniques. Both phosphines exhibit antibacterial activity against: *S. aureus*, *E. coli*, *K. pneumoniae* and *P. aeruginosa*, similar to ciprofloxacin and norfloxacin. They inhibit the growth of microorganisms in relatively low concentrations. Chalcogenides are slightly less active than phosphines and unmodified antibiotics. All the derivatives were also tested *in vitro* as anticancer agents towards mouse colon carcinoma (CT26) and human lung adenocarcinoma (A549). Cytotoxicity studies revealed that phosphines and their chalcogenides are able to inhibit the proliferation of the cells at relatively low concentrations. Moreover, all the tested compounds are more active against tested cell lines than cisplatin – the main representative of antitumor drugs.

Introduction

The large genetic variation of pathogenic organisms and the excessive frequency of antibiotics usage has resulted in the development of increasingly effective defence mechanisms by microorganisms. It has been recognized by the WHO as one of the most significant health dangers.[1,2] Although most bacteria have remained susceptible to the fluoroquinolones with MICs less than or equal to 1.0 μg ml^{-1}, low rates of resistance have been observed in some strains of *P. aeruginosa* and *Enterococci* and high rates in methicillin-resistant *S. aureus*. For this reason, the search for new antimicrobial agents is extremely important and desirable.

In our previous paper[3] we presented the spectroscopic profile and biological activity of ciprofloxacin (**HCp**) modified to a novel diphenylmethylphosphine derivative (Ph_2PCH_2Cp; **PCp**) and its oxide ($Ph_2P(O)CH_2Cp$; **OPCp**). The possibility of such a modification, benefiting from the presence of a secondary nitrogen atom in the piperazine ring of **HCp**,[4–6] seems to be especially attractive. This is confirmed by a number of papers showing that phosphines, as well as their derivatives and the metal complexes (*i.e.* copper, platinum, gold) exhibit promising anticancer, antibacterial or antiarthritic activities.[6–13]

Our studies have shown that **PCp** is able to inhibit the growth of microorganisms at the same level as **HCp**. Additional studies have revealed that this phosphine at higher concentrations is characterized by a lower *in vitro* toxicity against mammalian cells than the parent drug. Moreover, **PCp**, as previously shown for **HCp**, did not show any mutagenic activity and this was confirmed by testing its interactions with DNA.[3]

The results described above confirmed that this phosphine was a good choice for designing new biological agents. Therefore we decided to extend our studies. In this paper we present the syntheses, structures, spectroscopic properties, antibacterial and cytotoxic activities of a series of diphenylmethylphosphines and their chalcogenides derived from **HCp** and norfloxacin (**HNr**). Both drugs are 2nd generation fluorochinolones and are very similar to each other. They are broad-spectrum antibiotics, commonly used for the treatment of urinary tract, respiratory and digestive infections. **HCp** and **HNr** are active against gram-negative and some gram-positive bacteria. Most gram-negative bacteria, including non-fermentative bacteria such as *P. aeruginosa*, *Acinetobacter* spp.,

[a] *Faculty of Chemistry, University of Wrocław, ul. F. Joliot-Curie 14, 50-383 Wrocław, Poland. E-mail: malgorzata.jezowska-bojczuk@chem.uni.wroc.pl, radoslaw.starosta@chem.uni.wroc.pl; Tel: +48-71-3757281, +48-71-3757273*
[b] *Faculty of Chemistry, Jagiellonian University, R. Ingardena 3, 30-060 Kraków, Poland*
[c] *Department of Microbiology, Institute Genetics and Microbiology, University of Wroclaw, S. Przybyszewskiego str. 63/77, 51-148 Wroclaw, Poland*

† Electronic supplementary information (ESI) available: Crystal packing pictures, detailed NMR data, the selected photos of the cells after treatment with the tested compounds and cytotoxic assay curves for all presented compounds. CCDC 948747 (**OPCp·2CH_3COCH_3**), 948748 (**SPCp·0.5CH_2Cl_2**) and 948749 (**SePCp·0.79CH_3OH·0.11H_2O**). For ESI and crystallographic data in CIF or other electronic format see DOI: 10.1039/c3nj01243c

Burkholderia cepacia are highly susceptible *in vitro* and many gram-positive bacteria, including fastidious pathogens are susceptible or moderately susceptible.

The mechanism of their action is based on blocking the DNA replication process by binding gyrase or topoisomerase IV.[14–17] Moreover, recent studies have proved that **HCp** showed cytotoxic properties against a few tumour cell lines and decreased their viability *in vitro*.[18–20]

Results and discussion

Ph_2PCH_2-Nr (**PNr**) – a diphenylphosphine derivative of norfloxacin, similar to **PCp**,[3] was obtained as a result of a two-step one-pot synthesis from $Ph_2P(CH_2OH)_2Cl$. Chalcogenide derivatives: oxides (**OPCp**[3] and **OPNr**), sulfides (**SPCp** and **SPNr**) and selenides (**SePCp** and **SePNr**) were obtained from simple reactions of the corresponding phosphines with hydrogen peroxide, resublimed sulfur and metallic selenium, respectively (Fig. 1). The identities of all the compounds were confirmed using elemental analyses, ^{1}H, ^{31}P{^{1}H} and ^{13}C{^{1}H} NMR spectroscopy and mass spectrometry.

NMR spectroscopy of the phosphine chalcogenide derivatives

NMR spectra (see Experimental section and Table S1 in ESI†) were measured at room temperature in deuterated chloroform ($CDCl_3$) as a solvent. In the ^{31}P{H} NMR spectra both phosphines gave signals at −27.42 ppm (**PCp**)[3] and −27.50 ppm (**PNr**). The formation of the chalcogenide derivatives of these phosphines leads to significant changes in the spectra strongly shifting the signal of the phosphorus atom to lower fields. The biggest shift is observed for sulfide derivatives, and the chemical shift values are equal to 35.74 ppm for **SPCp** and 35.84 ppm for **SPNr**. The oxides give signals at 27.70 ppm for **OPCp**[3] and 27.36 ppm for **OPNr**, while the signals of phosphine selenides are placed at 26.11 ppm (**SePCp**) and 26.20 ppm (**SePNr**). Phosphorus–selenium coupling constants are equal to 726.5 and 731.4 Hz for **SePCp** and **SePNr**, respectively. They are significantly larger than those determined for selenides of tris(aminomethyl)phosphines ($P(CH_2NCH_2CH_2O)_3$: 709.8 Hz; $P(CH_2NCH_2CH_2NMe)_3$ and $P(CH_2NCH_2CH_2NEt)_3$: 707.5 Hz)[21] and other aliphatic phosphines (PMe_3:[22] 684.0 Hz, $P(t\text{-}Bu)_3$:[23] 693.0 Hz) and are comparable to the coupling constants determined for selenides of aromatic phosphines: (PPh_3:[22] 732.5 Hz).

The formation of chalcogenides does not cause significant changes in the position of the proton signals. The only noticeable changes are observed for $H^{1P'}$ protons from the P–CH_2–N group (Fig. 1) appearing as doublets (or broadened singlets for **SePCp** and **OPNr**). Formation of a P═X bond (X = chalcogenide) shifts this signal towards lower fields by 0.05–0.13 ppm in the case of oxides, 0.25 ppm for sulfides and 0.45–0.43 for selenides.

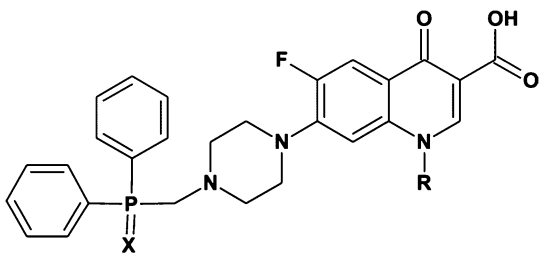

Fig. 1 Molecular structures of phosphines and their chalcogenides (X = oxygen, sulfur or selenium atom) derived from ciprofloxacin (R = cyclopropyl) and norfloxacin (R = ethyl).

In the ^{13}C{^{1}H} NMR spectra, analogously to the ^{1}H ones, the largest changes are observed for the $C^{1P'}$ atom and $C^{Ph(i)}$ – *ipso* carbon atom of the phenyl rings. A significant increase of the $^1J(C^{1P'}P)$ coupling constant is the most noticeable. The value of this constant is equal to 4.1 Hz for **PCp**, whereas for the oxide and the sulfide it is equal to 87.3 and 74.5 Hz, respectively. We did not observe a $C^{1P'}$ signal for **SePCp**. The $^1J(C^{1P'}P)$ coupling constant for **PNr** is 3.4 Hz and for its chalcogenides: 85.6, 72.7 and 66.3 Hz for **OPNr**, **SPNr** and **SePNr**, respectively. The signal for $C^{Ph(i)}$ is slightly shifted towards higher fields after the formation of a P═X bond with a simultaneous increase of the $^1J(C^{Ph(i)}P)$ coupling constant, wherein the changes of the constant value showed trends (12.4 and 11.7 Hz – **PCp** and **PNr**; 98.1 and 99.0 Hz – **OPCp** and **OPNr**; 79.0 and 79.0 Hz – **SPCp** and **SPNr**; 70.8 and 69.9 Hz – **SePCp** and **SePNr**;) like those observed for the $C^{1P'}$ carbon atom.

Summarizing, analysis of the NMR spectra suggests that regardless of the modified antibiotic we observed similar changes in the values of the chemical shifts and coupling constants for the derivatives of both ciprofloxacin and norfloxacin. This is fully justified because there is almost no difference between the molecules of both compounds.

X-ray structures

We obtained single crystals and resolved the X-ray structures of all three derivatives of **HCp**: **OPCp** in **OPCp**·$2CH_3COCH_3$, **SPCp** in **SPCp**·$0.5CH_2Cl_2$, and **SePCp** in **SePCp**·$0.79CH_3OH$·$0.11H_2O$. Selected crystallographic and data collection parameters are given in the Experimental section. Bond lengths and angles are summarized in Table 1. Perspective views of the molecules are depicted in Fig. 2.

As expected, all three molecules are similar to each other and to **PCp**,[3] they differ only by the chalcogenide atom bound to phosphorus. Detailed analysis indicates however that binding of the chalcogen causes significant changes in the geometry around the P atom: P–C bonds are shortened and C–P–C bond angles are enlarged. The largest changes are observed for **OPCp**, probably due to the most electronegative character of oxygen. Similar tendencies are observed also for other phosphines and their derivatives (*i.e.*: $P(CH_2NCH_2CH_2Y)_3$, where Y = O, NMe or NEt,[6,21] PMe_3,[24–26] PPh_3,[27–30] $P(t\text{-}Bu)_3$,[23] $P(CH_2CH_2CN)_3$,[31,32] 1,3,5-triaza-7-phosphaadamantane[33,34]).

A strong intramolecular hydrogen bond is observed in each one of the **OPCp**, **SPCp** and **SePCp** molecules, as for **PCp** (Table 1; O2–H2···O3). This bond does not involve the hydroxyl and carbonyl part of the same carboxyl group, but connects the OH part of the carboxyl group and the neighbouring carbonyl oxygen atom directly bound to the ring.

Despite their similar molecular structures, the presented derivatives crystallize in different crystal systems (see Fig. S1–S3 in ESI†) and are characterized by different intermolecular

Table 1 Selected bond lengths [Å] and angles [°] for **OPCp**, **SPCp** and **SePCp** together with **PCp**[3]

Geometry	PCp[3]	OPCp	SPCp	SePCp (A)	SePCp (B)
P(1)–X[a]		1.487(3)	1.959(1)	2.1094(10)	2.1088(12)
P(1)–C(31)	1.831(1)	1.806(4)	1.817(3)	1.825(3)	1.801(4)
P(1)–C(41)	1.839(1)	1.805(4)	1.826(3)	1.817(3)	1.802(4)
P(1)–C(1)	1.855(1)	1.821(4)	1.831(3)	1.842(4)	1.846(4)
F(12)–C(12)	1.359(1)	1.371(4)	1.363(3)	1.360(4)	1.355(4)
O(1)–C(20)	1.212(1)	1.215(5)	1.216(3)	1.219(5)	1.218(4)
O(2)–C(20)	1.336(1)	1.324(5)	1.320(3)	1.329(5)	1.327(4)
O(3)–C(17)	1.264(1)	1.258(5)	1.266(3)	1.251(4)	1.256(4)
Av. P(1)–C(1,31,41)	1.842(1)	1.811(4)	1.825(3)	1.828(3)	1.816(4)
Av. C(1,31,41)–P(1)–C(1,31,41)	100.49(5)	105.47(17)	104.64(13)	105.18(15)	106.23(17)
Hydr.bond O2–H2···O3					
O2···O3	2.551(2)	2.531(4)	2.533(3)	2.501(4)	2.510(4)
O2–H2, H2···O3	0.82, 1.79	0.82, 1.77	0.82, 1.77	0.84, 1.72	0.84, 1.73
O2–H2···O3	153.5	154.2	153.0	154.2	154.4

[a] X = O(4), S(1) or Se(1).

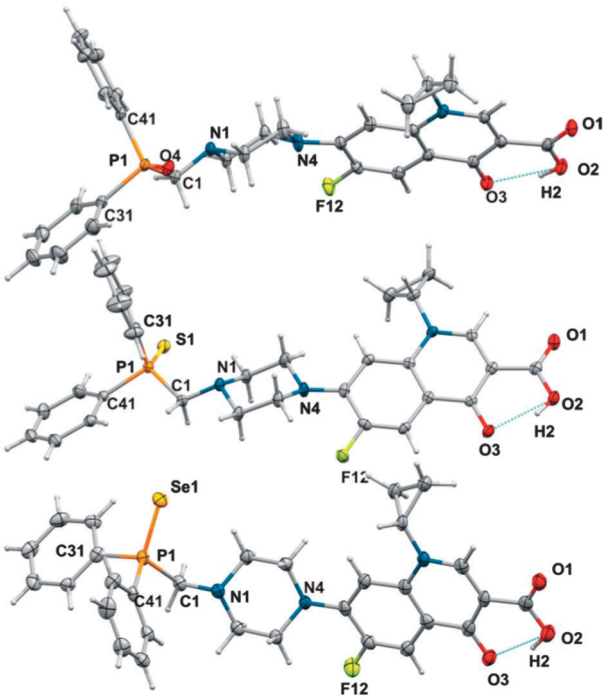

Fig. 2 The X-ray structures (50% ellipsoids) of **OPCp** (top), **SPCp** (middle) and the "A" molecule of **SePCp** (bottom).

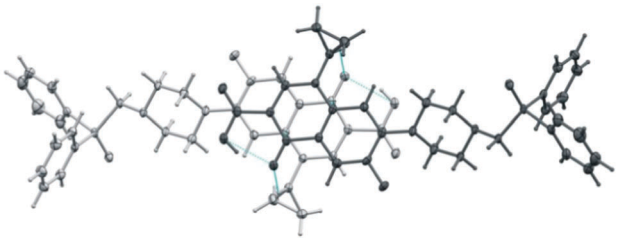

Fig. 3 Dimer of **OPCp** with π-stacking interaction between the quinolone rings (view perpendicular to the ring planes). The distance between the planes is equal to 3.291 Å.

interactions. **OPCp·2CH$_3$COCH$_3$** crystallizes in the triclinic system ($P\bar{1}$ space group). The elemental cell contains two molecules of **OPCp** and four solvent molecules. The solvent molecules are unconnected to the phosphine oxide therefore a high degree of observed structural disorder (see Fig. S1 in ESI†) is observed. **OPCp** molecules form dimers bound by strong π-stacking interactions which are typical for extended aromatic hydrocarbons[35] and show carbon atoms both overlapping with others and placed in the centers of the stacked rings (Fig. 3). **SPCp·0.5CH$_2$Cl$_2$** and **SePCp·0.79CH$_3$OH·0.11H$_2$O** crystallize in the monoclinic systems (both in the *P*21 space group). The elemental cell of **SPCp·0.5CH$_2$Cl$_2$** contains four molecules of phosphine sulfide (only one is independent) and two molecules of highly disordered molecules of occluded dichloromethane (see Fig. S2 in ESI†). On the other hand, the elemental cell of **SePCp·0.79CH$_3$OH·0.11H$_2$O** contains two pairs of independent molecules (A and B) differing not only in the selenide atom disorder (Fig. S3 in ESI†), but also in the geometry around the phosphorus atom. The crystal cell is also partially occupied by molecules of methanol and water connected to one another and to **SePCp** molecules by means of weak hydrogen bonds. Molecules of **SPCp** and **SePCp**, in comparison to **OPCp**, are connected in the crystal net only by weak interactions, mainly of C–H···π, C–H···O and C–H···S(Se) character. No classic π-stacking interactions are observed.

Antibacterial properties

The antibacterial activities of derivatives of fluorinated quinolones against a reference gram-positive strain of *S. aureus* ATCC 6538 and three gram-negative strains of *E. coli* ATCC 25922, *K. pneumoniae* ATCC 4352 and *P. aeruginosa* ATCC 27853 are presented in Table 3. The results of MICs and MBCs tests show various degrees of the bacterial susceptibility to the derivatives compared to their native forms (Kurskal–Wallis test, $P = 0.014$). The most of the examined compounds were bactericidal against the tested microorganisms, especially enteric gram-negative rods (*K. pneumoniae* and *E. coli*) (Kurskal–Wallis test, $P = 0.0017$). For **HCp** and all its derivatives the mean of the MICs and MBCs was in the range from 0.004 to 0.125 μg ml^{-1}

Table 2 Antibacterial activity of the investigated compounds against *Staphylococcus aureus* 6538, *Escherichia coli* 25922, *Klebsiella pneumoniae* 4352 and *Pseudomonas aeruginosa* 27853 strains. MIC – minimal inhibitory concentration, MBC – minimal bacteriocidal concentration

Cmpd	*S. aureus*	*E. coli*	*K. pneumoniae*	*P. aeruginosa*
	MIC [μg ml^{-1}]			
HCp	0.125	0.008	0.004	0.125
PCp	0.125	0.008	0.004	0.125
OPCp	1.0	1.0	0.125	16
SPCp	2.0	0.25	0.125	16
SePCp	0.5	0.0625	0.016	0.5
HNr	0.5	0.03	0.03	0.5
PNr	1.0	0.125	0.03	1.0
OPNr	2.0	2.0	0.25	16
SPNr	2.0	2.0	1.0	>16
SePNr	2.0	0.125	0.125	2.0
	MBC [μg ml^{-1}]			
HCp	0.25	0.008	0.008	0.25
PCp	0.25	0.016	0.008	0.25
OPCp	2.0	2.0	0.25	>16
SPCp	4.0	0.25	0.25	>16
SePCp	1.0	0.125	0.03	1.0
HNr	1.0	0.0625	0.03	1.0
PNr	1.0	0.125	0.0625	2.0
OPNr	2.0	2.0	0.5	>16
SPNr	4.0	4.0	1.0	>16
SePNr	4.0	0.25	0.25	4.0

and 0.004 to 16.0 μg ml^{-1}, respectively. Therefore, according to the recommendation of CLSI36 for **HCp**, in most cases the tested bacterial strains were susceptible to derivatives of **HCp** (Kurskal–Wallis test, P = 0.04). The mean of the MICs of the **HCp** derivatives was not greater than 1.0 μg ml^{-1}, except for that of **OPCp** for gram-positive *cocci* (with an intermediate susceptibility equal to 2.0 μg ml^{-1}) as well as that for **OPCp** and **SPCp** for non-fermentative rods of *P. aeruginosa* strain (Kurskal–Wallis test, P = 0.05). *P. aeruginosa* was resistant to these compounds with MICs of ≥16.0 μg ml^{-1} (Kurskal–Wallis test, P = 0.025).

It was found that the modification of native **HCp** by addition of a Ph_2PCH_2-group did not alter its antimicrobial activity (Table 2). **SePCp** was the most effective compound against all the tested bacteria, among the chalcogenated derivatives of **PCp**. The antibacterial activity of this compound was similar to the activity of **HCp** (Kurskal–Wallis test, P > 0.05). The MICs and MBCs of **SePCp** for gram-positive and gram-negative bacteria were in the range from 0.016 to 0.5 μg ml^{-1}, and 0.03 to 1.0 μg ml^{-1}, respectively. Notably, a high antibacterial activity for **OPCp** or **SPCp** was observed against enteric gram-negative bacteria (Kurskal–Wallis test, P = 0.045). For **SPCp** the MICs and MBCs were found to be ≤0.125 μg ml^{-1} and 0.25 μg ml^{-1} for *K. pneumoniae*, and ≤0.25 and 0.5 μg ml^{-1} for *E. coli*, respectively. For **OPCp** the mean of the MICs and MBCs were almost similar and were found to be ≤0.125 and 0.25 μg ml^{-1} for *K. pneumoniae*, and ≤1.0 and 2.0 μg ml^{-1} for *E. coli*, respectively. It should be noted that these derivatives were not effective against the *P. aeruginosa* strain (Kurskal–Wallis test, P = 0.048).

HNr the second investigated chemotherapeutic, also showed great antibacterial properties (Kurskal–Wallis test, P = 0.05). The mean of the MICs and MBCs of **HNr** and all its derivatives ranged from 0.03 to 0.5 μg ml^{-1} and 0.03 to 16.0 μg ml^{-1}, respectively. According to the recommendation of CLSI36 for **HNr**, almost all of the tested bacterial strains were susceptible to derivatives of **HNr**; their MICs were lower than 4.0 μg ml^{-1}. The only exception were gram-negative rods of *P. aeruginosa* resistant to **OPNr** and **SPNr** (Kurskal–Wallis test, P = 0.04) with MICs accounted ≥16.0 μg ml^{-1}.

Among all the derivatives of **HNr**, **PNr** and **SePNr** were characterized as the best antimicrobial agents against both gram-positive and gram-negative bacteria, including the *P. aeruginosa* strain. The mean of the MICs and MBCs of **PNr** were found to be in the range from 0.03 to 1.0 μg ml^{-1} and 0.0625 to 2.0 μg ml^{-1}, respectively. Whereas, the MICs and MBCs of **SePNr** were 0.125–2.0 μg ml^{-1} and 0.25–4.0 μg ml^{-1} range, respectively. Remarkably, the antibacterial activity of **OPNr** and **SPNr**, observed against gram-positive *cocci* and enteric gram-negative bacteria, were similar to the activity of **HNr** (Kurskal–Wallis test, P = 0.09). The values of the MICs and MBCs of **SPNr** were ≤2.0 and 4.0 μg ml^{-1} for *S. aureus* and *E. coli* and ≤1.0 and 1.0 μg ml^{-1} for *K. pneumoniae*, respectively. The mean of the MICs and MBCs of **OPNr** were almost similar and were ≤2.0 μg ml^{-1} and 2.0 μg ml^{-1} for *E. coli* and *S. aureus* and ≤0.25 μg ml^{-1} and 0.5 μg ml^{-1} for *K. pneumoniae*, respectively. These compounds were ineffective against *P. aeruginosa* strain (Kurskal–Wallis test, P = 0.045).

Cytotoxicity

To determine the cytotoxicity of the obtained derivatives we selected two cell lines, commonly used for preliminary *in vitro* tests: mouse colon carcinoma (CT26) and human lung adenocarcinoma (A549). A study of biological activity was undertaken with concentrations of the newly synthesized compounds ranging from 0.1 to 0.001 mM. In parallel, the influence of the widely used anticancer drug, cisplatin, was assessed. Treatment of CT26 and A549 cell lines with the tested compounds resulted in dose-dependent inhibition of cell proliferation. For both tested cell lines viability decreased with increasing concentration of the compounds. Fig. 4 and Fig. S8 and S9 in ESI† show the cytotoxic assays.

The obtained data indicates (Fig. 4) the statistically relevant differences in the cytotoxic action of the **HCp** and **HNr** derivatives. Generally, for both cell lines, all the tested compounds in our experimental system were found to have a higher cytotoxicity than cisplatin. Moreover, phosphines and all chalcogenides showed a much better anticancer effect than **HCp** (ANOVA/MANOVA, P = 0.00013) and **HNr** (ANOVA/MANOVA, P < 0.000001).

The best cytotoxic activity against the CT26 cell line was observed for sulfides and selenides. **SPCp** and **SePCp** at c = 0.01 mM induced a decrease of the cells viability by over 50% (Fig. 4A; ANOVA/MANOVA, P < 0.00005). Analogously, **SPNr** and **SePNr** at c = 0.01 mM decreased the cells viability by approx. 65 and 55% (Fig. 4B; ANOVA/MANOVA, P = 0.00002).

The A549 cell line was more resistant to the derivatives of **HCp**. **SPCp** and **SePCp** at c = 0.01 mM caused a 25% decrease of the cells viability, but **PCp** and **OPCp** at the same concentration – only 20% (Fig. 4C; ANOVA/MANOVA, P = 0.00002). Derivatives of **HNr** were much more cytotoxic. The highest activity was observed

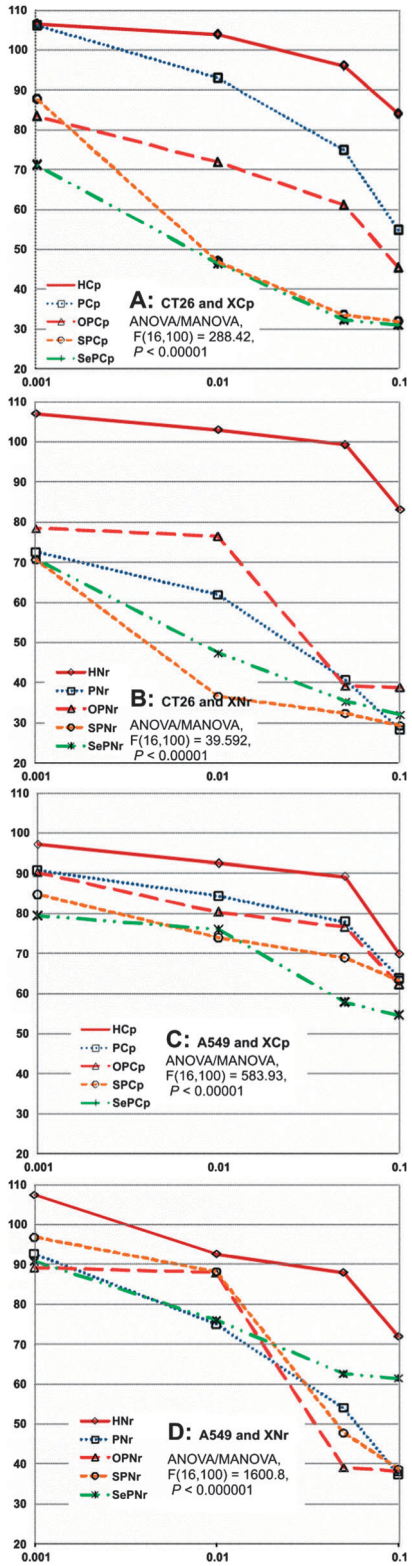

Fig. 4 Cytotoxic assay performed on CT26 and A549 cell lines for **HCp** and **HNr** and their derivatives. *X*-axis: the concentration of the compound [mM] presented in the logarithmic scale; *Y*-axis: surviving fraction.

for **OPNr** and **SPNr**, which caused respectively a 60 and 55% decrease of the viability at $c = 0.05$ mM (Fig. 4D; ANOVA/MANOVA, $P < 0.00005$). These two compounds lost their activity at $c = 0.01$ mM (ANOVA/MANOVA, $P > 0.05$) while **PNr** and **OPNr** decreased viability by 25% ANOVA/MANOVA, $P = 0.00002$).

Table 3 IC_{50} values [mM] for CT26 and A549 cells after treatment with the studied compounds for 4 hours, determined by MTT assay

Cmpd	IC_{50} c [mM]	
	CT26	A549
HCp	0.47 ± 0.05	0.38 ± 0.04
PCp	0.21 ± 0.07	0.35 ± 0.03
OPCp	0.22 ± 0.04	0.35 ± 0.03
SPCp	0.15 ± 0.02	0.44 ± 0.04
SePCp	0.17 ± 0.02	0.30 ± 0.03
HNr	0.47 ± 0.03	0.33 ± 0.05
PNr	0.16 ± 0.09	0.16 ± 0.04
OPNr	0.17 ± 0.02	0.15 ± 0.02
SPNr	0.18 ± 0.02	0.15 ± 0.02
SePNr	0.18 ± 0.02	0.32 ± 0.04
Cisplatin	2.20 ± 0.82	3.15 ± 0.45

The IC_{50} parameter values (Table 3) were determined from the fitting curve by calculating the concentration of a tested compound that reduces the surviving fraction in the treated cells by 50%, compared to control cells. For **HCp** and its derivative compounds against CT26 and A549 cell lines the IC_{50} values decreased in the following order: **SPCp** > **SePCp** > **PCp** ≈ **OPCp** ≫ **HCp** and **SePCp** > **OPCp** = **PCp** > **HCp** ≫ **SPCp** for the tested cell lines respectively. Analogously, the values of IC_{50} for **HNr** and its derivatives may be ordered as follows: **PNr** ≈ **OPNr** ≈ **SPNr** = **SePNr** ≫ **HNr** and **OPNr** = **SPNr** ≈ **PNr** ≫ **SePNr** ≈ **HNr** for CT26 and A549 cell lines, respectively.

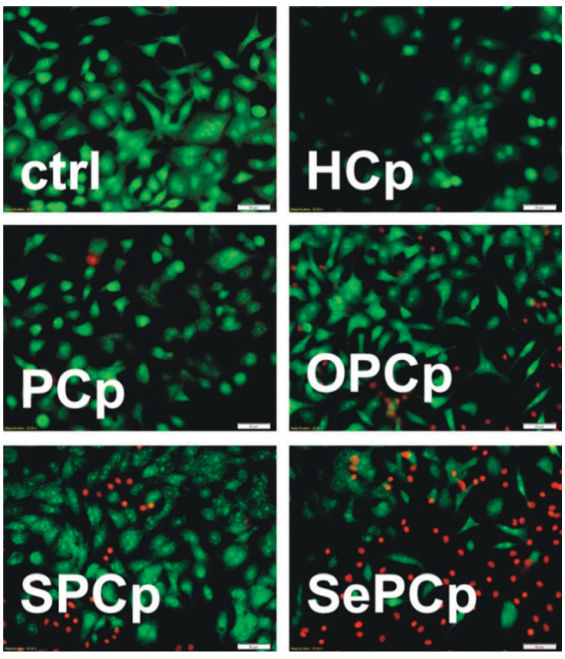

Fig. 5 Selected photos (magnification: 2000×; bar: 50 μm) of A549 cells after treatment with the tested compounds (0.05 mM) for 4 hours. The green cells with normal morphology are viable ones (AO^+), while round red cells are dead (PI^+).

Selected photographs of CT26 and A549 cells treated with the tested compounds are displayed in Fig. 5 (and Fig. S4–S8 in ESI†). The cell viability was examined by counting dead and alive cells stained with two fluorescent dyes: acridine orange (AO) and propidium iodide (PI). AO, in comparison ary to PI, penetrates into viable cells and binds to DNA by intercalation. PI due to its electric charge does not penetrate through the uninterrupted cytoplasmic membrane of viable and early apoptotic cells. Therefore, PI stains only cells with interrupted membranes – necrotic or late apoptotic ones. Accordingly, green cells with normal nuclei were treated as viable cells (AO^+), while red ones as dead cells (PI^+). As can be noticed in the presented photographs, the tested derivatives of **HCp** and **HNr** caused a significant reduction of the surviving fraction in both of the studied cell lines in comparison with the original antibiotics.

Conclusions

We synthesized a novel diphenylmethylaminophosphine derived from **HNr** and a series chalcogenide derivatives of this ligand as well as analogous derivatives of **HCp**. The identity and structure of the obtained new compounds were confirmed by elemental analysis, NMR, MS and X-ray techniques.

The antibacterial activity of the compounds was tested against *S. aureus* ATCC 6538, *E. coli* ATCC 25922, *K. pneumoniae* ATCC 4352 and *P. aeruginosa* ATCC 27853. The mean of the MICs of **PCp** and **PNr** were similar to those for **HCp** and **HNr**. Chalcogenide derivatives were found to be slightly less active, however selenides generally showed the highest antimicrobial activity among all of the derivatives. Their MBCs values were satisfactory, and were found to be 0.1 mg% for **SePCp** and 0.4 mg% for **SePNr**. Probably, the action mechanism of organoselenium compounds is based on the release of the cytoplasmic constituents from the cell and cell dehydration that could lead to disintegration. According to recent literature data such compounds, attached covalently to different biomaterials, inhibit the formation and growth of many bacterial biofilms.[37–39]

In vitro cytotoxicity studies showed that the investigated compounds exhibit potential anticancer properties. All of the tested derivatives of **HCp** and **HNr** were cytotoxic against human lung adenocarcinoma (A549) and mouse colon carcinoma (CT26) cell lines. For all of them we observed much better antitumor effect in comparison with the unmodified antibiotics. For example, the IC_{50} value for **HNr** was determined to be 0.47 mM for CT26 cell line and 0.33 mM for A549 cell line, while in the case of **OPNr** these values are 0.17 mM and 0.15 mM, respectively. In addition, the cytotoxicity of our compounds was much higher than that of cisplatin, the main representative of anticancer drugs.

The presented data are relevant in the context of further studies and even potential applications in therapy because we have proven that modification of **HCp** or **HNr** by the addition of the diphenylphosphinomethyl group as an interface to other functional moieties can selectively alter the biological activity of the parent drugs.

Now we are focusing on the synthesis and characteristics of copper(I) complexes obtained with phosphines. It is well known that phosphines are perfect binding ligands for this ion. Additionally, Cu(I) complexes are promising potential therapeutic agents with high anticancer activity.[7,40,41]

Experimental

Materials and methods

Reactions were carried out under a nitrogen atmosphere using standard Schlenk techniques. The reagents and solvents were purchased from Sigma-Aldrich and used without further purification. All the solvents were deaerated prior to use. $[PPh_2(CH_2OH)_2]^+Cl^-$ was synthesized according to the literature method.[42] **PCp** and **OPCp** were synthesized as described previously.[3]

NMR spectra were recorded on a Bruker Avance 500 MHz spectrometer with traces of solvent as an internal reference for ^1H and $^{13}C\{^1H\}$ spectra and 85% H_3PO_4 in H_2O as an external standard for $^{31}P\{^1H\}$. Chemical shifts are reported in ppm and coupling constants are reported in Hz. Mass spectra were registered on a Bruker Daltonics micrOTOF-Q Mass spectrometer equipped with an electrospray ionization (ESI) source and operated in the positive ion mode. Elemental analysis was performed with a Vario EL3 CHN analyzer.

Syntheses

S=PPh$_2$CH$_2$Cp (SPCp). The sulfide was obtained from the reaction of **PCp** (0.287 g; 0.542 mmol) in chloroform (25 cm^3) with equimolar amounts of resublimed sulfur (0.0174 g; 0.542 mmol). The mixture was placed in an ultrasonic bath for 0.5 h at room temperature. A yellowish solid was obtained after removing the solvent and purified by recrystallization from the chloroform–methanol mixture (1 : 2 V : V). The obtained microcrystals were dried for 24 h under vacuum to remove any occluded solvent molecules.

Yield 87%. Anal. calcd for $C_{30}H_{29}FN_3O_3PS$ (561.6): C, 64.15; H, 5.16; N, 7.48%. Found: C, 64.12; H, 5.23; N, 7.45%. NMR ($CDCl_3$, 298 K): $^{31}P\{^1H\}$: 35.74 s; ^1H: H^{3Pb}: 14.98 s, H^{2P}: 8.66 s, H^{5P}: 7.90 d J = 13.00, $H^{Ph(o),(m),(p)}$: 7.94–7.45, H^{8P}: 7.28 d J = 7.2, H^{1Pa}: 3.08 q J = 3.4, $H^{3P'}$: 3.24 m, $H^{1P'}$: 3.54 d J = 5.0, $H^{4P'}$: 2.91 m, H^{1Pb}: 1.38 q J = 7.3, H^{1Pb}: 1.15 td J = 6.7; 3.2; $^{13}C\{^1H\}$: C^{4P}: 176.93 s, C^{3Pa}: 166.85 s, C^{6P}: 154.52 d J = 251.6; C^{2P}: 147.29 s, C^{7P}: 145.60 d J = 10.0, C^{9P}: 138.96 s, $C^{Ph(i)}$: 131.83 d J = 79.0, $C^{Ph(o)}$: 131.73 d J = 2.7, $C^{Ph(p)}$: 131.62 d J = 9.0, $C^{Ph(m)}$: 128.53 d J = 11.8, C^{10P}: 119.63 d J = 7.3, C^{5P}: 112.16 d J = 22.7, C^{3P}: 107.93 s, C^{8P}: 104.81 d J = 2.7, $C^{1P'}$: 61.51 d J = 74.5, $C^{4P'}$: 54.73 d J = 7.3, $C^{3P'}$: 49.61 d J = 5.4, C^{1Pa}: 35.26 s, C^{1Pb}: 8.17 s. MS ($CHCl_3$): 562.2 $[MH]^+$ 100%.

Se=PPh$_2$CH$_2$Cp (SePCp). An equimolar mixture of **PCp** (0.321 g; 0.607 mmol) and metallic selenium (0.048 g; 0.608 mmol) in chloroform (25 cm^3) was placed in an ultrasonic bath for 3 h. A yellowish solid was deposited at −18 °C. It was filtered off and then purified by recrystallization from the chloroform–methanol mixture (1 : 2 V : V). The obtained solid was dried for 24 h under vacuum.

Yield 86%. Anal. calcd for $C_{30}H_{29}FN_3O_3PSe$ (608.5): C, 59.21; H, 4.76; N, 6.91%. Found: C, 59.19; H, 4.79; N, 6.87%. NMR ($CDCl_3$, 298 K): $^{31}P\{^1H\}$: 26.11 ^1J(PSe) = 726.5; ^1H: H^{3Pb}: 14.97s, H^{2P}: 8.74 s, H^{5P}: 7.94 d J = 13.0, $H^{Ph(o),(m),(p)}$: 7.98–7.48, H^{8P}: 7.30 d J = 7.1, H^{1Pa}: 3.52 qn.t J = 4.0; 3.1, $H^{3P'}$: 3.27, $H^{1P'}$: 3.74* s, $H^{4P'}$: 2.90, H^{1Pb}: 1.39 q J = 3.90, H^{1Pb}: 1.19 td J = 6.7; 3.6; $^{13}C\{^1H\}$: C^{4P}: 177.06 s, C^{3Pa}: 166.92 s, C^{6P}: 154.57 d J = 251.6, C^{2P}: 147.40 s, C^{7P}: 145.58 d J = 10.9, C^{9P}: 139.00 s, $C^{Ph(i)}$: 130.48 d J = 70.8, $C^{Ph(o)}$: 131.88 d J = 2.7, $C^{Ph(p)}$: 132.23 d J = 9.1, $C^{Ph(m)}$: 128.60 d J = 11.8, C^{10P}: 119.89 d J = 8.2, C^{5P}: 112.39 d J = 23.6, C^{3P}: 108.12 s, C^{8P}: 104.84 d J = 2.70, $C^{1P'}$: 62.04 d J = 65.95, $C^{4P'}$: 54.63 d J = 5.4, $C^{3P'}$: 49.47 d J = 4.5, C^{1Pa}: 35.26 s, C^{1Pb}: 8.24 s. MS ($CHCl_3$): 610.1 $[MH]^+$ 100%.

PPh_2CH_2Nr (**PNr**): A solution of 0.8853 g of $[PPh_2(CH_2OH)_2]^+Cl^-$ (3.13 mmol) in 25 cm^3 of methanol was placed in an ice bath, NEt_3 (4 ml) was added dropwise. After 30 min of stirring **HNr** (1.0 g; 3.13 mmol) was added. Then the mixture was stirred for 1.5 h at room temperature. The obtained white solid was centrifuged, washed twice with water and dried under reduced pressure.

Yield 89%. Anal. calcd for $C_{29}H_{29}FN_3O_3P$ (517.2): C, 67.34; H, 5.61; N, 8.13%. Found: C, 67.31; H, 5.63; N, 8.11%. NMR ($CDCl_3$, 298 K): $^{31}P\{^1H\}$: −27.50 s; ^1H: H^{3Pb}: 15.13 s, H^{2P}: 8.63 s, H^{5P}: 7.95 d J = 13.0, $H^{Ph(o),(m),(p)}$: 7.46–7.33, H^{8P}: 6.82 d J = 6.8, H^{1Pa}: 4.31 m, $H^{3P'}$: 3.36 m, $H^{1P'}$: 3.29 d J = 2.8, $H^{4P'}$: 2.89 m, H^{1Pb}: 1.56 m; $^{13}C\{^1H\}$: C^{4P}: 176.96 s, C^{3Pa}: 167.26 s, C^{6P}: 154.57 d J = 252.5; C^{2P}: 147.13 s, C^{7P}: 146.15 d J = 10.6, C^{9P}: 137.21 s, $C^{Ph(i)}$: 138.09 d J = 11.7, $C^{Ph(o)}$: 132.91 d J = 18.2, $C^{Ph(p)}$: 128.82 s, $C^{Ph(m)}$: 128.58 d J = 6.6, C^{10P}: 120.39 d J = 7.7, C^{5P}: 112.61 d J = 23.2, C^{3P}: 108.27 s, C^{8P}: 103.95 d J = 3.2, $C^{1P'}$: 61.27 d J = 3.4, $C^{4P'}$: 54.15 d J = 9.0, $C^{3P'}$: 49.98 d J = 4.3, C^{1Pa}: 49.82 s, C^{1Pb}: 14.51 s. MS ($CHCl_3$): 518.2 $[MH]^+$ 100%; 443.2 2%; 332.1 $[CH_2Nr]^+$ 36%.

O═PPh_2CH_2Nr (**OPNr**): The oxide derivative was prepared in the reaction of **PNr** (0.108 g; 0.209 mmol) with an equimolar amount of H_2O_2 (30% solution in water) in chloroform (25 cm^3). After 3 h of stirring at room temperature the solution was left at −18 °C overnight. The precipitated white solid was filtered and purified by recrystallization from the chloroform–methanol mixture (1 : 2 V : V). The obtained solid was dried for 24 h under reduced pressure.

Yield 84%. Anal. calcd for $C_{29}H_{29}FN_3O_4P$ (533.2): C, 65.32; H, 5.44; N, 7.88%. Found: C, 65.27; H, 5.47; N, 7.87%. NMR ($CDCl_3$, 298 K): $^{31}P\{^1H\}$: 27.34 s; ^1H: H^{3Pb}: 15.07 s, H^{2P}: 8.67 s, H^{5P}: 8.03 d J = 13.1, $H^{Ph(o),(m),(p)}$: 7.84–7.49, H^{8P}: 6.81 d J = 6.9, H^{1Pa}: 4.31 q J = 7.2, $H^{3P'}$: 3.33 m, $H^{1P'}$: 3.42 s*, $H^{4P'}$: 3.01 m, H^{1Pb}: 1.57 t J = 7.2; $^{13}C\{^1H\}$: C^{4P}: 176.98 s, C^{3Pa}: 167.16 s, C^{6P}: 154.45 d J = 251.6, C^{2P}: 147.12 s, C^{7P}: 145.79 d J = 10.0, C^{9P}: 137.05 s, $C^{Ph(i)}$: 132.08 d J = 99.0, $C^{Ph(o)}$: 132.16 d J = 2.7, $C^{Ph(p)}$: 131.10 d J = 9.1, $C^{Ph(m)}$: 128.71 d J = 10.9, C^{10P}: 120.69 d J = 7.4, C^{5P}: 112.78 d J = 22.7, C^{3P}: 108.39 s, C^{8P}: 103.92 d J = 2.7, $C^{1P'}$: 60.85 d J = 85.6, $C^{4P'}$: 54.88 d J = 7.9, $C^{3P'}$: 49.59 d J = 4.5, C^{1Pa}: 49.71 s, C^{1Pb}: 14.44 s. MS ($CHCl_3$): 534.2 $[MH]^+$ 100%; 332.1 $[CH_2Nr]^+$ 5.5%.

S═PPh_2CH_2Nr (**SPNr**): A chloroform solution (25 cm^3) containing an equimolar amount of **PNr** (0.250 g; 0.483 mmol) and resublimed sulfur (0.0155 g; 0.483 mmol) was placed in an ultrasonic bath for 0.5 h at room temperature. The yellowish solid of sulfide derivative was filtered and purified by recrystallization from the chloroform–methanol solution (1 : 2 V : V). The obtained white microcrystals were dried for 24 h under vacuum.

Yield 87%. Anal. calcd for $C_{29}H_{29}FN_3O_3PS$ (549.3): C, 63.41; H, 5.28; N, 7.65%. Found: C, 63.38; H, 5.31; N, 7.62%. NMR ($CDCl_3$, 298 K): $^{31}P\{^1H\}$: 35.84 s; ^1H: H^{3Pb}: 15.10 s, H^{2P}: 8.62 s, H^{5P}: 7.93 d J = 13.0, $H^{Ph(o),(m),(p)}$: 7.95–7.44, H^{8P}: 6.77 d J = 6.9, H^{1Pa}: 4.08 m, $H^{3P'}$: 3.21 m, $H^{1P'}$: 3.54 d J = 5.0, $H^{4P'}$: 2.83 m, H^{1Pb}: 1.54 t d J = 7.2; $^{13}C\{^1H\}$: C^{4P}: 176.78 s, C^{3Pa}: 167.03 s, C^{6P}: 154.32 d J = 252.5, C^{2P}: 146.99 s, C^{7P}: 145.79 d J = 10.9, C^{9P}: 136.99 s, $C^{Ph(i)}$: 131.76 d J = 79.0, $C^{Ph(o)}$: 131.65 d J = 2.7, $C^{Ph(p)}$: 131.55 d J = 9.1, $C^{Ph(m)}$: 128.46 d J = 11.8, C^{10P}: 120.32 d J = 8.2, C^{5P}: 112.43 d J = 23.6, C^{3P}: 108.09 s, C^{8P}: 103.85 d J = 3.6, $C^{1P'}$: 61.52 d J = 72.7, $C^{4P'}$: 54.68 d J = 7.3, $C^{3P'}$: 49.68 d J = 4.5, C^{1Pa}: 49.66 s, C^{1Pb}: 14.38 s. MS ($CHCl_3$): 550.2 $[MH]^+$ 100%; 332.1 $[CH_2Nr]^+$ 2.5%.

Se═PPh_2CH_2Nr (SePNr). The selenide derivative was prepared by reacting PNr (0.281 g; 0.543 mmol) with an equimolar amount of metallic selenium (0.0429 g; 0.543 mmol) in chloroform (25 cm^3). The mixture was placed in an ultrasonic bath for 3 h. A yellowish solid was deposited at −18 °C. It was filtered and purified by recrystallization from the chloroform–methanol solution (1 : 2 V : V). The obtained microcrystals were dried for 24 h under vacuum.

Yield 85%. Anal. calcd for $C_{29}H_{29}FN_3O_3PSe$ (596.5): C, 58.39; H, 4.86; N, 7.05%. Found: C, 58.34; H, 4.90; N, 7.07%. NMR ($CDCl_3$, 298 K): $^{31}P\{^1H\}$: 26.30 ^1J(PSe) = 731.4; ^1H: H^{3Pb}: 15.06 s, H^{2P}: 8.64 s, H^{5P}: 7.99 d J = 13.0, $H^{Ph(o),(m),(p)}$: 8.00–7.47, H^{8P}: 6.78 d J = 6.94, H^{1Pa}: 4.30 q J = 7.2, $H^{3P'}$: 3.24 m, $H^{1P'}$: 3.72 d J = 4.0, $H^{4P'}$: 2.87 m, H^{1Pb}: 1.57 t J = 7.3; $^{13}C\{^1H\}$: C^{4P}: 176.77 s, C^{3Pa}: 167.02 s, C^{6P}: 154.31 d J = 251.6, C^{2P}: 146.99 s, C^{7P}: 145.77 d J = 10.0, C^{9P}: 136.98 s, $C^{Ph(i)}$: 130.39 d J = 69.9, $C^{Ph(o)}$: 131.75 d J = 2.7, $C^{Ph(p)}$: 132.14 d J = 9.1, $C^{Ph(m)}$: 128.47 d J = 11.8, C^{10P}: 120.34 d J = 8.2, C^{5P}: 112.44 d J = 23.6, C^{3P}: 108.10 s, C^{8P}: 103.85 d J = 2.7, $C^{1P'}$: 61.79 d J = 66.3, $C^{4P'}$: 54.61 d J = 6.4, $C^{3P'}$: 49.64 d J = 4.5, C^{1Pa}: 49.73 s, C^{1Pb}: 14.39 s. MS ($CHCl_3$): 598.1 $[MH]^+$ 100%.

X-ray structures. The data were collected at 293 or 100 K using an Oxford Cryosystem device on a Kuma KM4CCD κ-axis diffractometer with graphite-monochromated Mo Kα radiation generated from a diffraction X-ray tube operated at 50 kV and 20 mA. Data reduction and analysis were carried out with the Oxford Diffraction programs.[43,44] The structures were analysed by direct methods (program SHELXS97[45]) and refined by the full-matrix least-squares method on all F^2 data using the SHELXL97[45] program. Non H atoms were included in the refinement, with anisotropic displacement parameters and the H atoms were included from the geometries of the molecules. The data for **SePCp·0.79CH_3OH·0.11H_2O** were corrected for absorption,[44] min/max absorption coefficients were 0.6634/0.8436. In the solution of the **OPCp·2CH_3COCH_3** structure there is a very large maximum of electron density (2.21 e $Å^{-3}$) close to one of the highly disordered molecules of occluded solvent (d(Q1–C1S) = 1.431, d(Q1–O1S) = 1.803 Å).

Crystal/refinement data. **OPCp·2CH$_3$COCH$_3$** $\equiv$ $C_{36}H_{41}FN_3O_6P$; M_r = 661.69, crystal size: 0.15 × 0.09 × 0.07 mm, crystal system: triclinic, space group: $P\bar{1}$, unit cell: a = 8.650(2) Å, b = 12.440(2) Å, c = 16.140(3) Å, α = 105.39(2)°, β = 90.16(2)°, γ = 94.95(2)°; V = 1667.6(6) Å^3, D_{calcd}(Z = 2) = 1.318 g cm^{-3}, θ range for data collection: 2.91–25.00°, Mo Kα radiation (λ = 0.71073 Å), μ_{Mo} = 0.139 mm^{-1}, reflections collected/unique 17 054/5882 [R_{int} = 0.0294], final R indices [$I > 2\sigma(I)$] R_1 = 0.0858, wR_2 = 0.2339, R indices (all data) R_1 = 0.0986, wR_2 = 0.2435, GOF = 1. 041, largest diff. peak and hole: 2.208 (*this large maximum of electron density is placed close to one of the highly disordered molecules of occluded acetone solvent*) and −0.738 e Å^{-3}, data/restraints/parameters: 5882/0/444; T = 293(2) K.

SPCp·0.5CH$_2$Cl$_2$ $\equiv$ $C_{30.50}H_{29}ClFN_3O_3PS$; M_r = 603.05, crystal size: 0.20 × 0.11 × 0.07 mm, crystal system: monoclinic, space group: $P21$, unit cell: a = 8.748(1) Å, b = 22.372(3) Å, c = 14.514(2) Å, β = 94.60(2)°, V = 2831.4(6) Å^3, D_{calcd}(Z = 4) = 1.415 g cm^{-3}, θ range for data collection: 2.28–25.00°, Mo Kα radiation (λ = 0.71073 Å), μ_{Mo} = 0.310 mm^{-1}, reflections collected/unique 19 067/4988 [R_{int} = 0.0470], final R indices [$I > 2\sigma(I)$] R_1 = 0.0539, wR_2 = 0.1465, R indices (all data) R_1 = 0.0701, wR_2 = 0.1528, GOF = 1.322, largest diff. peak and hole: 0.720 and −1.235 e Å^{-3}, data/restraints/parameters: 4988/0/365; T = 293(2) K.

SePCp·0.79CH$_3$OH·0.11H$_2$O $\equiv$ $C_{30.79}H_{32.36}FN_3O_{3.89}PSe$; M_r = 635.58, crystal size: 0.33 × 0.15 × 0.13 mm, crystal system: monoclinic, space group: $P21$, unit cell: a = 8.102(3) Å, b = 25.993(6) Å, c = 14.216(4) Å, β = 92.42(3)°, V = 2991.2(16) Å^3, D_{calcd}(Z = 4) = 1.411 g cm^{-3}, θ range for data collection: 2.75–28.78°, Mo Kα radiation (λ = 0.71073 Å), μ_{Mo} = 1.355 mm^{-1}, T_{min} = 0.6634, T_{max} = 0.8436, reflections collected/unique 18 670/11 096 [R_{int} = 0.0268], final R indices [$I > 2\sigma(I)$] R_1 = 0.0396, wR_2 = 0.0810, R indices (all data) R_1 = 0.0470, wR_2 = 0.0844, GOF = 1.026, largest diff. peak and hole: 0.810 and −0.441 e Å^{-3}, data/restraints/parameters: 11 096/0/757; flack parameter: −0.001(5); T = 100(2) K.

The antimicrobial activity studies

Strains and bacterial suspensions. The antimicrobial activity of **HCp** and **HNr** and their derivatives was tested at concentrations from 0.002 μg ml^{-1} to 16.0 μg ml^{-1} against the reference bacterial strains from the American Collections ATCC: *Escherichia coli* ATCC 25922, *Staphylococus aureus* ATCC 6538, *Klebsiella pneumoniae* ATCC 4352 and *Pseudomonas aeruginosa* ATCC 27853. The bacterial strains, provided by the Institute of Genetics and Microbiology University of Wroclaw, were cultured aerobically at 34 °C in nutrient agar (0.5% enzyme-hydrolyzed proteins, 0.3% meat extract, 0.5% NaCl, 1.5% agar–agar) overnight and then three to four colonies of each of the strains were suspended in 0.85% of NaCl solution to produce stock preparations containing a log-phase cell density of approximately 108 CFU per ml (colony forming units per milliliters). Each of the bacterial suspensions was diluted in physiologic salt solution to 1 : 1000 (10^5 CFU per ml).[46]

Determination of MIC and MBC. The minimum inhibitory concentration (MIC), defined as the lowest concentration of material that inhibits the growth of an organism, was determined based on the broth dilution susceptibility tests. MIC values were determined using the dilution of microarrays recommended by CLSI.[46] 96-well microtiter plates were filled with 100 μl of liquid LB (1% yeast extract, 1% tryptone, 0.5% NaCl) medium containing serial dilutions of the tested compounds. All of the substances were diluted in DMSO to prepare 32.0 mg ml^{-1} stocks solutions. The bacterial suspensions (10 μl) were added into each well of the microtiter plates with the exception of the control and the plates were incubated aerobically for 16–18 h at 34 °C. As a positive control a suspension of bacteria in an LB broth medium was used, for the negative control a pure LB broth medium was used and the blank control was a suspension of bacteria in physiologic salt solution. Each control and dilution of tested compounds were tested in triplicate. The MIC values were determined visually and spectrophotometrically. The OD (optical density) of each well was measured at λ = 590 nm using an automatic 96-well microplate reader Asys Hitachi 340, Driver version: 4.02 (Biogenet, Poland). MICs were taken as the lowest concentrations not showing any visible growth or their values of absorbance in the bacterial cultures after incubation were less than or equal to the blank control.

The minimum bactericidal concentration (MBC), *i.e.*, the lowest concentration of a substance that kills 99.9% of the bacteria was also determined from the dilution of microarrays. For growth inhibitory concentration (MIC) the presence of viable microorganisms was tested and the lowest concentration causing a bactericidal effect was reported to be the MBC. The MBC was determined by removing a 10 μl volume of the medium from each microtiter plate well used for MIC determinations and spotting onto nutrient agar. Agar plates were incubated aerobically for 18–24 h at 34 °C. The concentration causing a bactericidal effect was selected based on the absence of colonies on the agar plate. For each test 3 replicates were undertaken.

The mean values of MICs and MBCs were interpreted as antimicrobial activity according to the recommendation of the CLSI.[36]

Statistical analysis

The antimicrobial activity of the studied derivatives was compared to their native forms (**HCp**, **HNr**) by nonparametric analysis of variance (Kruskal–Wallis ANOVA by ranks or Median test). The ANOVA (using STATISTICA for Windows; StatSoft, Tulsa, OK, USA) was used to test for significant difference of the mean of the MICs and MBCs between bacterial strains. The P values less than or equal to 0.05 indicate that the values being compared are statistically significantly different at a 95% confidence level.

Cytotoxicity studies

Cell cultures. CT26 cell line (mouse colon carcinoma, morphology: fibroblast, ATCC: CRL-2638) and A549 cell line (human lung adenocarcinoma, morphology: epithelial, ATCC: CCL-185) were obtained from Professor Luis G. Arnaut's group (Chemistry Department, University of Coimbra, Portugal). Cells were cultured in Dulbecco's Modified Eagle Medium (DMEM) without phenol red, supplemented with 10% fetal bovine serum (FBS) and with 1% streptomycin/penicillin. Cultures were

incubated at 37 °C in a humidified atmosphere containing 5% CO_2 (standard conditions). Cells were passaged at preconfluent density, using a solution containing 0.05% trypsin and 0.5 mM EDTA. All cell culture fluids were purchased from IMMUNIQ (Poland).

Cytotoxicity assay. Cells were seeded in the 96-well plate at a density of 10 000 cells per ml and incubated for 24 h under standard conditions. After that time, the culture medium was changed for the tested compounds at a final concentration of 0.1–0.001 mM in PBS (IMMUNIQ, Poland). Cells with compounds were incubated for 4 h, then washed with PBS and finally a new medium was added. After 24 h of incubation the cytotoxicity was assessed.

The cytotoxicity of the tested compounds was determined by the MTT assay. Briefly, 200 μl of MTT (5 mg ml^{-1}, Sigma-Aldrich) was added to each of the wells and incubated for 4 h at room temperature. Then the blue formazan reaction product formed was dissolved in 100 μl of DMSO–CH_3OH mixture (1/1; v/v). The absorbance of the formazan solution was measured at 565 nm using an Infinite 200M PRO NanoQuant plate reader (Tecan, Switzerland).

The results were determined as a cell survival fraction, S/S_0 (%) and were calculated using the formula: S/S_0 (%) = [abs_{565nm} of treated cells/abs_{565nm} of untreated cells (control)] × 100. Untreated cells, cultured only in medium, were treated as a control. IC_{50} values (concentration of the tested agent causing 50% inhibition of cell growth) were calculated from the constructed dose–response curve presenting the effect of different concentrations and cell surviving fraction after treatment with the studied compounds. All data are represented as the mean values of three independent experiments.

Fluorescence microscopy. Viable and dead cells were detected by staining with acridine orange (AO, 5 mg L^{-1}) and propidium iodide (PI, 5 mg L^{-1}) for 20 min and examined using a fluorescence inverted microscope (Olympus IX51, Japan) with an excitation filter of 470/20 nm. Photographs of the cells after treatment with the tested compounds were taken under a magnification of 20×.

Statistical analysis. For the determination of the significant difference between the percentage of survival rate of cell lines in the presence of the studied compounds at their various concentrations the Tukey HSD test of ANOVA/MANOVA (using STATISTICA for Windows; StatSoft, Tulsa, OK, USA) was used. The numbers of colony-forming units per culture (CFU) from the biological assays were converted to percentage survival values, where the inoculum of eukaryotic cells in the control sample without the tested chemiotherapeutic agents was set at 100% and values for the survival rates were expressed as % CFU. *P* values less than or equal to 0.05 indicate that the values compared are statistically significantly different at a 95% confidence level.

Acknowledgements

The authors gratefully acknowledge financial support from the Polish National Science Centre (grant 2011/03/B/ST5/01557). The *in vitro* research was carried out with the equipment purchased thanks to the financial support of the European Regional Development Fund in the framework of the Polish Innovation Economy Operational Program (contract no. POIG.02.01.00-12-023/08).

Notes and references

1 World Health Organization. The evolving threat of antimicrobial resistance – Options for actions 2012 (WHO/IER/PSP/2012.2).
2 G. Alvan, C. Edlund and A. Heddini, *Drug Resist. Updates*, 2011, **14**, 70–76.
3 A. Bykowska, R. Starosta, A. Brzuszkiewicz, B. Bażanów, M. Florek, N. Jackulak, J. Król, J. Grzesiak, K. Kaliński and M. Jeżowska-Bojczuk, *Polyhedron*, 2013, **60**, 23–29.
4 H. Coates, P. A. T. Hoye, *US Pat.*, 3 035 053, 1962.
5 A. A. Karasik, I. O. Georgiev, E. I. Musina, O. G. Sinyashin and J. Heinicke, *Polyhedron*, 2001, **20**, 3321–3331.
6 R. Starosta, M. Florek, J. Król, M. Puchalska and A. Kochel, *New J. Chem.*, 2010, **34**, 1441–1449.
7 C. Marzano, M. Pellei, F. Tisato and C. Santini, *Anti-Cancer Agents Med. Chem.*, 2009, **9**, 185–211.
8 S. J. Berners-Price and P. J. Sadler, *Bioinorg. Chem.*, 1988, **70**, 27–102.
9 R. Starosta, K. Stokowa, M. Florek, J. Król, A. Chwiłkowska, J. Kulbacka, J. Saczko, J. Skała and M. Jeżowska-Bojczuk, *J. Inorg. Biochem.*, 2011, **105**, 1102–1108.
10 F. J. Ramos-Lima, A. G. Quiroga, J. M. Perez, M. Font-Bardia, X. Solans and C. Navarro-Ranninger, *Eur. J. Inorg. Chem.*, 2003, 1591–1598.
11 K. Neplechova, J. Kasparova, O. Vrana, O. Novakova, A. Habtemarian, B. Watchman, P. J. Sadler and V. Brabec, *Mol. Pharmacol.*, 1999, **56**, 20–30.
12 W. Henderson and S. R. Alley, *Inorg. Chim. Acta*, 2001, **322**, 106–112.
13 C. F. Shaw, *Chem. Rev.*, 1999, **99**, 2589–2600.
14 P. M. Hawkey, *J. Antimicrob. Chemother.*, 2003, **51**, 29–35.
15 D. C. Hopper, *Drugs*, 1999, **58**, 6–10.
16 K. Drlica, *Curr. Opin. Microbiol.*, 1999, **2**, 504–508.
17 B. D. Bax, P. F. Chan, D. S. Eggleston, A. Fosberry, D. R. Gentry, F. Gorrec, I. Giordano, M. M. Hann, A. Hennessy, M. Hibbs, J. Huang, E. Jones, J. Jones, K. Koretke Brown, C. J. Lewis, E. W. May, M. R. Saunders, O. Singh, C. E. Spitzfaden, C. Shen, A. Shillings, A. J. Theobald, A. Wohlkonig, N. D. Pearson and M. N. Gwynn, *Nature*, 2010, **466**, 935–940.
18 T. Kloskowski, N. Gurtowska and T. Drewa, *Pulm. Pharmacol. Ther.*, 2010, **23**, 373–375.
19 T. Kloskowski, N. Gurtowska, M. Nowak, R. Joachimiak, A. Bajek, J. Olkowska and T. Drewa, *Acta Physica Polonica B*, 2011, **42**, 859–865.
20 D. J. Smart, D. Halicka, F. Traganos, Z. Darzynkiewicz and G. M. Williams, *Cancer Biol. Ther.*, 2008, **7**, 113–119.
21 R. Starosta, B. Bażanów and W. Barszczewski, *Dalton Trans.*, 2010, **39**, 7547–7555.
22 K. D. Cooney, T. R. Cundari, N. W. Hoffman, K. A. Pittard, M. D. Temple and Y. Zhao, *J. Am. Chem. Soc.*, 2003, **125**, 4318–4324.

23 H.-U. Steinberger, B. Ziemer and M. Meisel, *Acta Crystallogr., Sect. C: Cryst. Struct. Commun.*, 2001, **57**, 323–324.
24 L. S. Bartell and L. O. Brockway, *J. Chem. Phys.*, 1960, **32**, 512–515.
25 C. J. Wilkins, K. Hagen, L. Hedberg, Q. Shan and K. Hedberg, *J. Am. Chem. Soc.*, 1975, **97**, 6352–6358.
26 E. J. Jacob and S. Samdal, *J. Am. Chem. Soc.*, 1977, **99**, 5656–5663.
27 B. J. Dunne and A. G. Orpen, *Acta Crystallogr., Sect. C: Cryst. Struct. Commun.*, 1991, **47**, 345–347.
28 C. P. Brock, W. B. Schweizer and J. D. Dunitz, *J. Am. Chem. Soc.*, 1985, **107**, 6964–6970.
29 X.-P. Zhou, W.-X. Ni, S.-Z. Zhan, J. Ni, D. Li and Y.-G. Yin, *Inorg. Chem.*, 2007, **46**, 2345–2347.
30 P. G. Jones, C. Kienitz and C. Thone, *Z. Kristallogr.*, 1994, **209**, 80–81.
31 F. A. Cotton, D. J. Darensbourg, M. F. Fredrich, W. H. Ilsley and J. M. Troup, *Inorg. Chem.*, 1981, **20**, 1869–1872.
32 A. J. Blake, R. A. Howie and G. P. McQuillian, *Acta Crystallogr., Sect. B: Struct. Crystallogr. Cryst. Chem.*, 1981, **37**, 1959–1962.
33 R. E. Marsh, M. Kapon, S. Hu and F. H. Herbstein, *Acta Crystallogr., Sect. B: Struct. Sci.*, 2001, **58**, 62–77.
34 S. Otto, A. Ionescu and A. Roodt, *J. Organomet. Chem.*, 2005, **690**, 4337–4342.
35 C. Janiak, *J. Chem. Soc., Dalton Trans.*, 2000, 3885–3896.
36 Clinical, Laboratory Standards Institute. Performance Standards for antimicrobial susceptibility testing twenty-third informational supplement. CLSI Document M100-S23, CLSI Wayne, PA, January, 2013.
37 O. Wang and T. J. Webster, *J. Biomed. Mater. Res., Part A*, 2012, **100A**, 3205–3210.
38 P. Tran, A. Hamood, T. Mosley, T. Gray, C. Jarvis, T. Webster, B. Amaechi, T. Enos and T. Reid, *J. Dent. Res.*, 2013, **92**, 461–466.
39 P. Tran, A. Hamood, T. Mosley, J. Cortez, T. Gray, J. Colmer-Hamood, M. Shashtri, J. Spallholtz, A. Hammod and T. Reid, *Appl. Environ. Microbiol.*, 2009, **75**, 3586–3592.
40 C. Marzano, M. Pellei, S. Alidori, A. Brossa, G. Lobbia, F. Tisato and C. Santini, *J. Inorg. Biochem.*, 2006, **100**, 299–304.
41 C. Marzano, V. Gandin, M. Pellei, D. Colavito, G. Papini, G. Lobbia, E. Del Giudice, M. Porchia, F. Tisato and C. Santini, *J. Med. Chem.*, 2008, **51**, 798–808.
42 J. Fawcett, P. A. T. Hoye, R. D. W. Kemmitt, D. J. Law and D. R. Russell, *J. Chem. Soc., Dalton Trans.*, 1993, 2563–2568.
43 CrysAlis CCD, Oxford Diffraction, 2009.
44 CrysAlis RED, Oxford Diffraction, 2009.
45 G. M. Sheldrick, *Acta Crystallogr., Sect. A: Found. Crystallogr.*, 2007, **64**, 112–122.
46 Clinical, Laboratory Standards Institute. Methods for dilution antimicrobial susceptibility tests for bacteria that aerobically Approved Standard- seventh edition. CLSI Document M7-A7, CLSI Wayne, PA, January, 2006.